Acta Pharmacologica Sinica (2013) 34: 271–281
 1671-4083/13 $32.00
www.nature.com/aps

Original Article

1-Oxoeudesm-11(13)-eno-12,8a-lactone induces G_2/M arrest and apoptosis of human glioblastoma cells *in vitro*

Shan-shan LIU[1, 2], Yan-feng WANG[2], Li-sha MA[1], Bei-bei ZHENG[1], Lin LI[1], Wei-dong XIE[1], Xia LI[1, 2, *]

[1]*School of Ocean, Shandong University, Weihai 264209, China;* [2]*School of Pharmaceutical Sciences, Shandong University, Ji-nan 250012, China*

Aim: To investigate the effects of 1-oxoeudesm-11(13)eno-12,8a-lactone (OEL), a novel eudesmane-type sesquiterpene isolated from *Aster himalaicus*, on the cell cycle and apoptosis in human glioblastoma cells *in vitro*.
Methods: Human malignant glioblastoma cell lines U87 and A172 were used. The cytotoxicity of OEL was examined using the MTT assay. Cell apoptosis was assessed with DAPI staining and flow cytometry. DNA damage was determined by measuring the phosphorylation of H2AX using immunofluorescence staining and Western blotting. Cell cycle profiles were measured with flow cytometry. The mRNA expression of p53 and p21Waf1/Cip1 was investigated using real-time PCR. The protein expression of γ-H2AX, caspase-9, caspase-3, p53, p21Waf1/Cip1, cyclin B1, and cdc2 was analyzed with Western blotting.
Results: Treatment of the malignant glioblastoma cells with OEL inhibited the cell growth in dose- and time-dependent manners (the values of IC_{50} at 48 and 72 h were 29.5 and 16.99 μmol/L, respectively, in U87 cells; 7.2 and 9.5 μmol/L, respectively, in A172 cells). OEL (10–30μmol/L) induced apoptosis and G_2/M phase arrest in both U87 and A172 cells. OEL induced the phosphorylation of cdc2, a G_2/M phase cyclin-dependent kinase, and decreased the expression of cyclin B1 required for progression through the G_2/M phase in U87 cells. The compound remarkably increased the phosphorylation of H2AX in U87 cells. Moreover, OEL increased the mRNA and protein levels of p53 and its target gene $p21^{Waf1/Cip1}$ in U87 cells. The compound also induced p53 phosphorylation. Pretreatment with PFT-α, a specific inhibitor of p53 transcriptional activity, could partially reverse the inhibition of OEL on the viability of U87 and A172 cells.
Conclusion: OEL suppresses the growth of human glioblastoma cells *in vitro* via inducing DNA damage, p53-mediated cell cycle arrest and apoptosis, thus warrants further studies as a lead compound of anti-glioblastoma drug.

Keywords: 1-oxoeudesm-11(13)-eno-12,8a-lactone; *Aster himalaicus*; malignant glioma; apoptosis; cell cycle arrest; DNA damage; p53; PFT-α

Acta Pharmacologica Sinica (2013) 34: 271–281; doi: 10.1038/aps.2012.137; published online 19 Nov 2012

Introduction

Malignant gliomas, the most common primary brain tumors, are aggressive, difficult to treat, and have a very poor prognosis. The median survival of patients with malignant gliomas is less than 15 months, even in selected clinical trial populations and with the use of multimodal therapy, including surgery, radiotherapy, and chemotherapy[1]. The key reasons for the failure of chemotherapy in malignant gliomas are the rapid proliferation of cancer cells, frequent acquisition of drug-resistant phenotypes and the occurrence of secondary malignancies[2, 3]. In addition, the benefit of chemotherapy on patient prognosis in advanced malignant gliomas remains to be determined. Therefore, the development of new drugs for the treatment of malignant glioma is an important and urgent concern.

Apoptosis is an evolutionarily conserved and orchestrated cell-death process that is characterized by membrane blebbing, shrinking of the cytoplasm, DNA fragmentation, and the formation of distinct apoptotic bodies that contain components of the dying cell. This process also represents a major mechanism of action induced by chemotherapeutics to combat cancer cells[4, 5]. Studies have demonstrated that chemotherapy and γ-irradiation primarily kill cancer cells by inducing apoptosis[6, 7]. Therefore, the development of new anti-cancer drugs that induce apoptosis in tumor cells is an attractive strategy and an important goal for the field of cancer

* To whom correspondence should be addressed.
E-mail xiali@sdu.edu.cn
Received 2012-03-21 Accepted 2012-08-26

research[8–10].

Chemicals that interfere with cell cycle progression have been attracting increasing attention in cancer research. The division of eukaryotic cells is a highly regulated process[11]. The activation of a highly conserved family of protein kinases, such as cyclin-dependent kinases (CDKs), mediates tumor progression through the cell cycle. The activation of CDKs requires binding to cyclins, which are regulatory subunits. These cyclin/CDK complexes are universal cell cycle regulators, with each complex controlling a specific transition between phases of the cell cycle.

Natural plants products are a valuable source of novel compounds that can be utilized to combat tumor cells. Various drugs, such as taxane, vinca alkaloids, and hydroxycamptothecin, are derived from herbal plants and exhibit excellent anti-proliferative activity against cancer cells[12, 13]. The *Aster* (*Compositae*) genus is composed of approximately 250 species of plants. More than 20 aster species have been used in traditional Chinese medicine to treat snakebites, fever, cold, tonsillitis, and pneumonia[14]. In the present study, we examined 1-oxoeudesm-11(13)-eno-12,8a-lactone (OEL), a novel, eudesmane-type sesquiterpene compound isolated from the Chinese herb, *Aster himalaicus*, which we described in our previous report[14]. We also investigated the anti-cancer activity and mechanisms of action of OEL in the human malignant glioma cell lines, U87 and A172.

Materials and methods

Chemicals and reagents

The structure of OEL, isolated from *Aster himalaicus*, was identified by spectral data, as previously described[14] (Figure 1A). Purified OEL (>98%) was dissolved in dimethylsulfoxide (DMSO) at 10 mmol/L as a stock and diluted as necessary, according to experimental requirements.

3-(4,5-dimethylthiazol)-2,5-diphenyltetrazolium bromide (MTT) and 4′,6-diamidino-2-phenylindole (DAPI) were purchased from Sigma Co, USA. Fetal bovine serum (FBS) and Dulbecco's modified Eagle's medium (DMEM) were obtained from GIBCO BRL (Gaithersburg, MD). All other chemicals were commercial products of reagent grade.

The stock solution of OEL was prepared at a concentration of 10 mmol/L in DMSO and was stored at -20 °C until use. For all the experiments, the final concentration of the test compound was prepared by diluting the stock with DMEM. Control cultures received the carrier solvent (0.1% DMSO).

Cell lines and cell culture

U87 and A172 (with wide-type p53), U251 (with mutant p53), and Saos-2 (with deficient p53) cells were kindly provided by Dr Bing YAN and Dr Changjun ZHU of Shandong University. Normal cell lines, including a human hepatocyte cell line (HL7702), a rat cardiomyocyte cell line (H9C2) and a mouse embryo fibroblast *cell* line (3T3), were obtained from the Shanghai Institute for Biological Sciences (SIBS), Chinese Academy of Sciences (China). All the cell lines were maintained in DMEM (Gibco, Invitrogen) or RPMI-1640 (Hyclone) medium supplemented with 10% FBS, 100 units/mL of penicillin G, and 100 μg/mL of streptomycin in a humidified atmosphere of 37 °C and 5% CO_2.

Cytotoxicity assay

The cytotoxicity of OEL was assessed using the MTT assay. Cells were cultured at a density of 5×10^3 cells/well in 96-well plates (Costar, Cambridge, Massachusetts, USA) overnight. Twenty-four hours later, cells were treated with vehicle or PFT-α at the indicated concentrations for 1 h prior to the administration of OEL for the indicated time periods. Then, 20 μL of MTT (5 g/L) was added to each well and incubated for 4 h at 37 °C. The IC_{50} values (concentration resulting in 50% inhibition of cell growth) were calculated by plotting the results relative to untreated cells, which were considered to be 100%. Each experiment was performed in triplicate.

Immunofluorescence staining

Cells were seeded onto 12-mm round, glass cover slips in 24-well plates. Zero to 6 h after OEL treatment, cells were fixed with cold methanol: acetone (1:1) for 5 min, washed twice with cold PBS, and permeabilized in 0.1% Triton X-100 for 10 min. To prevent non-specific antibody binding, the cells were incubated with 3% goat serum. The cover slips were

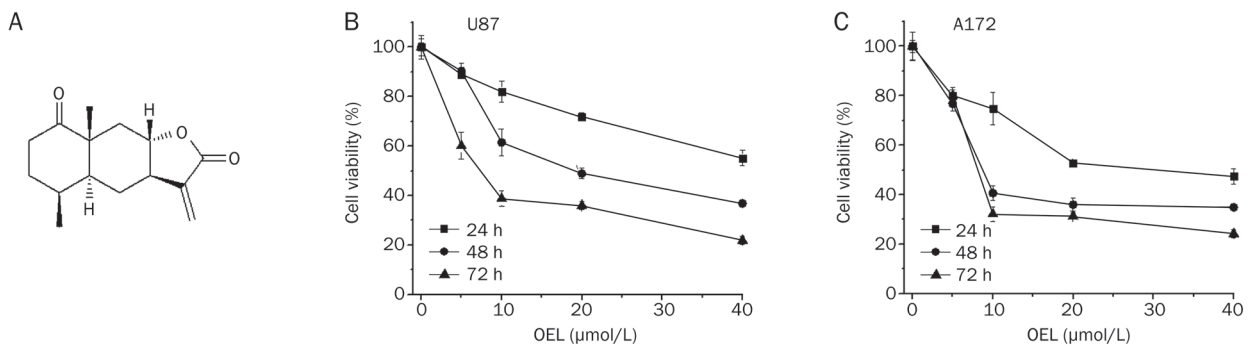

Figure 1. (A) Chemical structure of 1-oxoeudesm-11(13)eno-12,8a-lactone (OEL). (B, C) U87 and A172 cells were treated with OEL (5 μmol/L to 40 μmol/L) for 24 h to 72 h. Cell viability was denoted as a percentage of the untreated control (OEL 0 μmol/L) at the concurrent time point. Data are expressed as the mean±SD of triplicate experiments.

then incubated with the anti-phospho-H2AX antibody for 2 h, washed in PBS, and incubated with TRITC-conjugated goat anti-rabbit secondary antibody for 1 h at room temperature. Then, the cells were washed in PBS three times and counterstained with DAPI. Fluorescence images were captured under a confocal microscope[15].

Analysis of apoptosis by flow cytometry

The BD Pharmingen™ Annexin V:FITC Apoptosis Detection Kit was used to evaluate apoptosis. Cells were seeded at a density of 3×10^4 cells/mL into 6-well plates. After 24 h incubation, the cells were treated with various concentrations of OEL and incubated for an additional 24 h. At the indicated time points, the cells were washed twice with ice-cold PBS and trypsinized. Then, 100 μL of each cell sample was transferred to individual tubes and centrifuged at 200×*g* for 5 min. The supernatant was removed, and the cells were resuspended in 100 μL of Annexin V-FITC binding buffer and incubated at room temperature in the dark for 15 min with 5 μL Annexin V-FITC. Next, 5 μL of propidium iodide (PI; 50 mg/L) was then added for 5 min. In accordance with the manufacturer's instructions, the apoptotic ratio was analyzed by flow cytometry (Becton Dickinson, USA)[16] and WinMDI 2.9 software. Annexin V-positive cells were considered apoptotic.

RNA extraction and relative quantification by real-time PCR

Total RNA was extracted using the RNAeasy kit according to the manufacturer's instructions (Bioecon Biotec Co Ltd, China). The purity of RNA was measured by calculating the $OD_{260/280}$ of the RNA samples (>1.8). cDNA was synthesized via reverse transcription using M-MLV Reverse Transcriptase and Oligo (dT) primers. The expression levels of the p53 and $p21^{Waf1/Cip1}$ genes were detected using real-time-PCR assays. PCR amplification was performed in triplicate, in an 8-tube strip format (Axygen, Union City, CA), using a Mastercycler ep realplex apparatus (Eppendorf, Germany). Each reaction contained 1×SYBR Green PCR Master mix, 1 μL forward primer and reverse primer and 1 μL template cDNA in a final volume of 20 μL. The following primers were used to detect p53 and $p21^{Waf1/Cip1}$ gene expression, respectively: sense: 5′-TAACAGTTCCTGCATGGGCGGC-3′ and antisense: 5′-AGGACAGGCACAAACACGCACC-3′, product size of 121 bp; sense: 5′-CACTCCAAACGCCGGCTGATCTTC-3′ and antisense: 5′-TGTAGAGCGGGCCTTTGAGGCCCTC-3′, product size of 101 bp[17]. The following primers were used to detect the GAPDH gene, which served as a control for the total amount of RNA: sense: 5′-CCA TGG AGA AGG CTG GGG -3′ and antisense: 5′-CAA AGT TGT CAT GGA TGA CC-3′. Amplification was performed for 45 cycles of sequential denaturation (95 °C, 2 min), annealing (60 °C, 15 s) and extension (72 °C, 20 s). Data acquisition and the analysis of real-time PCR assay were performed using the Mastercycler ep realplex. Each fluorescent reporter signal was measured against the internal reference dye signal to normalize for non-PCR-related fluorescence fluctuations between wells. For all samples, real-time PCR was performed in three independent experiments. All primers were synthesized by Sangon Co, Ltd (Shanghai, China).

Cell cycle distribution by flow cytometric analysis

Cells were seeded into 6-well plates and then treated with varying concentrations of OEL. After the designated time intervals, cells were detached with trypsin and collected by centrifugation, followed by washing, fixation, and PI staining. The cell cycle distribution was examined by flow cytometry, and the data were analyzed using the Modfit program (Becton Dickinson, USA).

Western blot analysis

The protein from whole cell lysates was analyzed by Western blot. Samples were boiled with 1×Laemmli buffer, subjected to 12% SDS-polyacrylamide gel electrophoresis and transferred to nitrocellulose membranes. The membranes were washed in distilled water and then blocked with 5% non-fat milk in TBS-T buffer (10 mmol/L Tris-HCl, 150 mmol/L NaCl, and 0.05% [*v*/*v*] Tween-20; pH 7.8) for at least 1 h at room temperature. After a short wash in TBS-T buffer, the membranes were incubated in a solution containing monoclonal antibodies specific for caspase-9, p53, p21 (Santa Cruz Biotechnology, Inc, USA), cleaved caspase-3, GAPDH, γ-H2AX (Cell Signal Technology, USA), cyclin B1, cdc2, p-cdc2 (Thr14 and Tyr15) (Bioworld Technology, Inc, USA) for at least 2 h at room temperature or overnight at 4 °C. Membranes were then incubated with a biotin-conjugated goat anti-mouse IgG or anti-rabbit IgG secondary antibody (diluted 1:1000; Santa Cruz Biotechnology, Inc, USA). Proteins were visualized using the enhanced chemiluminescence detection system (ECL®, Amersham Biosciences).

Statistical analysis

All experiments were performed at least three times. Statistical analysis was performed with analysis of variance (ANOVA), followed by Turkey's *t*-test. *P*-values of <0.05 were considered statistically significant.

Results

OEL inhibits cell survival in human glioblastoma cells

We performed an MTT colorimetric assay to assess the cytotoxic effect of OEL on the human glioblastoma cell proliferation. Two human glioblastoma cell lines (U87 and A172) were treated with OEL for 24 h to 72 h. OEL treatment caused remarkable growth inhibition in a dose- and time-dependent manner (Figure 1B and 1C) in both U87 and A172. The IC_{50} of OEL at 48 h and 72 h in U87 cells was 29.5 and 16.99 μmol/L, respectively, and in A172 cells was 7.2 and 9.5 μmol/L, respectively.

Additionally, we tested the effects of OEL on two additional cancer cell lines (U251 and Saos-2) and three normal cell lines (HL7702, H9C2, and 3T3). As shown in Table 1, OEL inhibited the growth of U251 and Saos-2 cells, and OEL was less cytotoxic to normal cell lines compared to these cancer cell lines. The IC_{50} of OEL at 48 h in HL7702, H9C2, and 3T3 cells was

45.89, 75.31, and 73.02 μmol/L, respectively (Table 1).

Table 1. Cytotoxicity of OEL in cancer cells (U87, A172, U251, and Saos-2) and normal cells lines (HL7702, H9C2, and 3T3). The effects of OEL on cancer cells and normal cells were examined by MTT assay. The cells were treated with various concentrations of OEL for 48 h. The IC_{50} values of OEL were then calculated. Data are expressed as the mean±SD of three independent experiments.

Cell lines	IC_{50} (μmol/L) for 48 h
U87	29.50
A172	7.2
U251	31.90
Saos-2	34.62
HL7702	45.89
H9C2	75.31
3T3	73.02

The effects of OEL on cancer cells and normal cells lines. The cells were treated with various concentrations of OEL for 48 h and examined by MTT method. The IC_{50} values of OEL were then calculated. Data from three independent experiments.

OEL induces apoptotic effect in U87 and A172 cells

To characterize the cell growth inhibition in response to OEL, we monitored changes in the morphology of U87 cells. Compared to the controls, OEL treatment induced marked morphologic alterations that are associated with apoptosis, including cell shrinkage and granular apoptotic bodies (Figure 2A).

Flow cytometry was used to quantitatively analyze apoptosis in U87 cells via dual staining with FITC-Annexin V and propidium iodide (PI). Flow cytometric analysis revealed that the proportion of cells stained with Annexin V increased in the OEL-treated cells in a dose-dependent manner. The percentages of Annexin V-positive cells following treatment with 0 μmol/L to 30 μmol/L OEL for 24 h were 8.9%, 14.8%, 18.9%, and 46.7% (U87) and 1.4%, 16.8%, 35.7%, and 47.3% (A172) (Figure 2B and 2C).

OEL induces G_2/M phase arrest in U87 and A172 cells

After exposure to different concentrations of OEL for the indicated time intervals, we used flow cytometry to examine the cell cycle and determine whether OEL exerted its inhibitory effect via the induction of cell cycle arrest in addition to apoptosis. OEL altered the cell cycle distribution of both U87

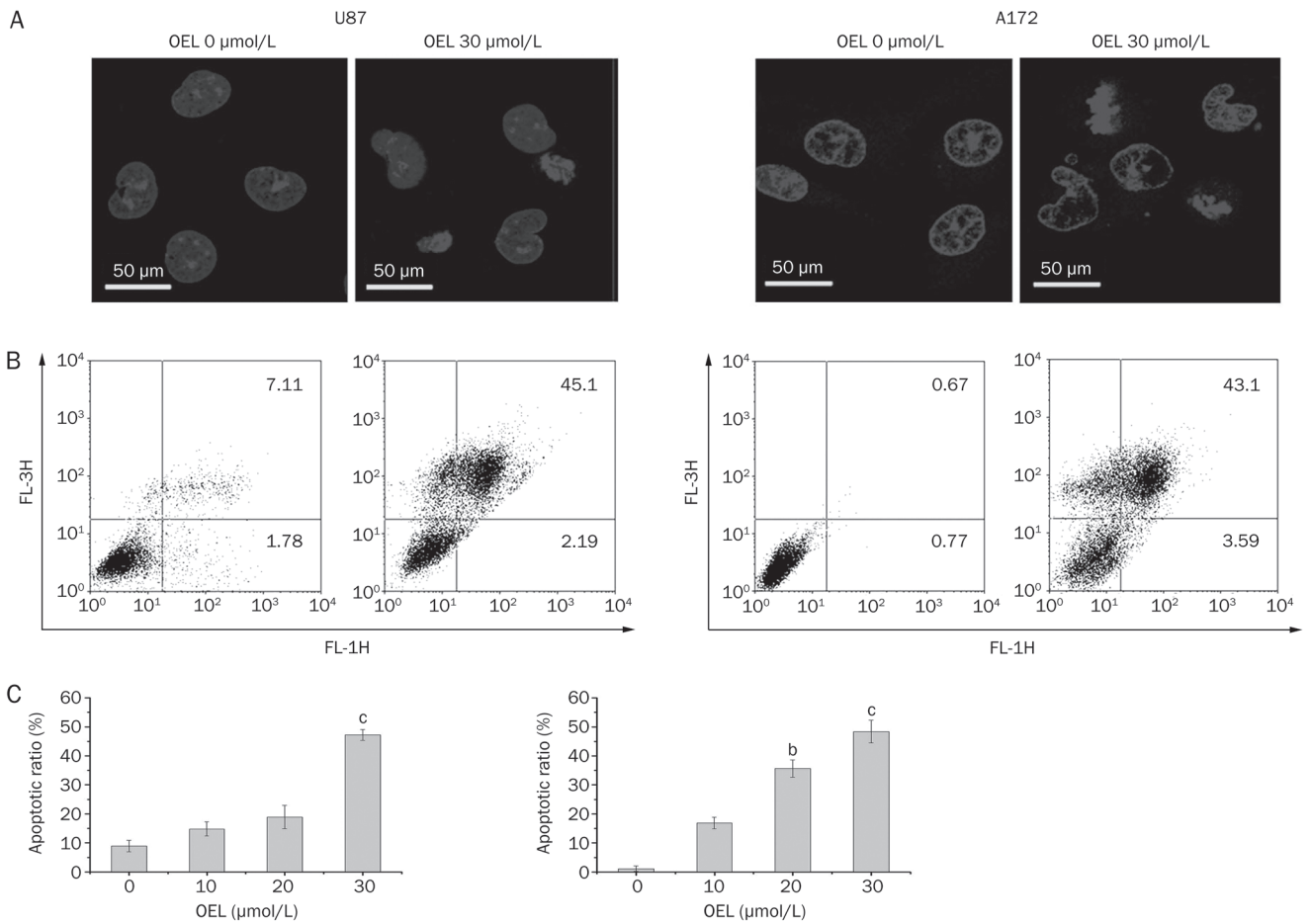

Figure 2. OEL-induced apoptosis was observed in U87 and A172 cells. Cells were treated with OEL (0, 10, 20, and 30 μmol/L) for 24 h. (A) Fluorescence micrographs of untreated and OEL-treated U87 and A172 cells after DAPI staining; magnification: ×63. (B, C) Quantification of OEL-induced apoptosis in U87 and A172 cells using flow cytometric analysis. $^{b}P<0.05$, $^{c}P<0.01$ compared with control (OEL, 0 μmol/L) group.

and A172 cells (Figure 3A and 3C). The percentage of cells in G_2/M phase increased with a concomitant reduction of cells in G_0/G_1 phase. The proportion of cells arrested in G_2/M phase was remarkably increased at higher concentrations of OEL (20 and 30 μmol/L) in U87 cells. Next, we analyzed the cell cycle profile of U87 cells treated with OEL for 48 and 72 h. In the absence of OEL, only 2.06% of U87 cells were in G_2/M phase (Figure 3C). By contrast, there was a significant accumulation of U87 cells in G_2/M after OEL treatment for 48 h (19.9%) and 72 h (27.6%). Compared to untreated cells, there was a dramatic increase in the sub-G_1 population after OEL treatment for 48 h. This result suggests that OEL, preceding the induction of apoptosis, induced G_2/M phase arrest. Hence, these results demonstrate that OEL induces cell cycle arrest in G_2/M phase, followed by apoptosis in a dose- and time-dependent manner.

Cell cycle proteins and caspase activation are involved in OEL-induced G_2/M phase arrest and apoptosis

Next, Western blotting was used to analyze cell cycle regulatory proteins involved in G_2/M phase, including cyclin B1, cdc2, and phosphorylated cdc2 (p-cdc2), in U87 cells after treatment with 10 to 30 μmol/L of OEL for 24 h. In response to OEL treatment, we observed a reduction in cyclin B1 expression and the induction of cdc2 phosphorylation (Thr14 and Tyr15), whereas the absolute protein level of cdc2 was unaffected (Figure 4A).

U87 cells were treated with various concentrations of OEL for 24 h, and caspase-9 and caspase-3 activities were determined by Western blotting. OEL promoted the activation of caspase-9 and caspase-3 (Figure 4B) in a dose-dependent manner. These results indicate that OEL-induced apoptosis is caused by the activation of caspase-9 and -3 in U87 cells.

OEL induces DNA damage in human glioblastoma cells

DNA damage triggers cell cycle arrest and apoptosis[18]. To elucidate the possible mechanisms of OEL-induced G_2/M arrest and apoptosis, we assessed changes in the phosphorylation of H2AX (γ-H2AX) in OEL-treated U87 cells. H2AX, a variant form of histone H2A, becomes phosphorylated (γ-H2AX) at serine 139 in response to DNA double-strand breaks[19]. Compared with untreated cells, OEL treatment increased H2AX phosphorylation after 2 h, as determined by immunofluorescence staining and immunoblot analysis

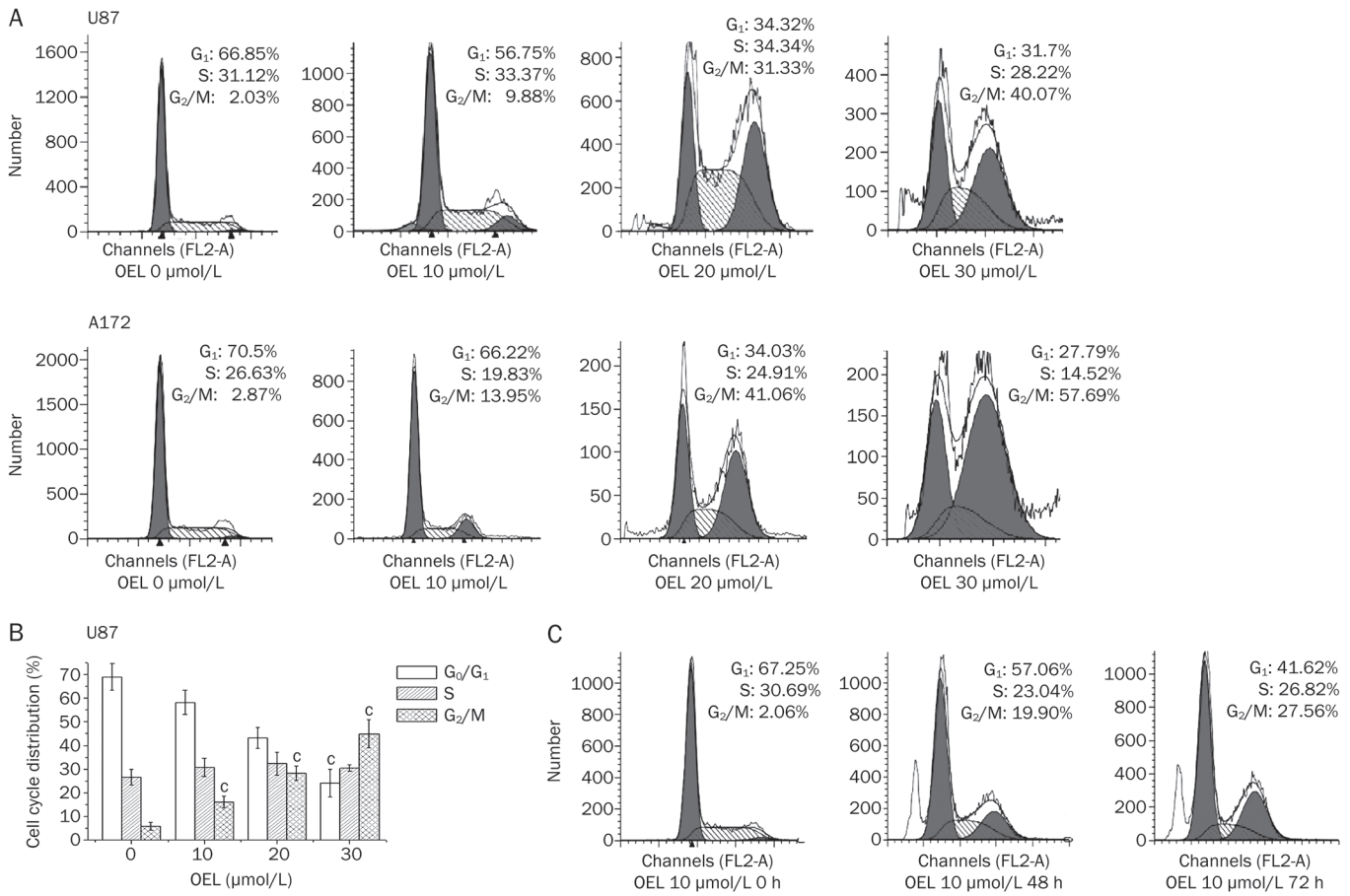

Figure 3. OEL induced cell cycle arrest in G_2/M phase. (A) Cells were treated with various concentrations of OEL (0–30 μmol/L) for 24 h, and the cell cycle profile was assessed using flow cytometry. Representative cell cycle profiles of U87 and A172 cells. (B) Representative histograms of the cell cycle distribution of U87 cells treated with OEL for 24 h. Data are shown as the mean±SD of four independent experiments. $^cP<0.01$ compared with control (OEL, 0 μmol/L) group. (C) Cell cycle patterns of U87 cells treated with OEL for 0, 48, and 72 h by flow cytometric analysis.

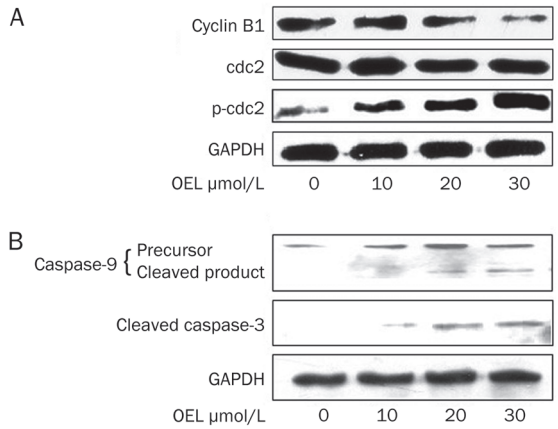

Figure 4. Western blot analysis of cell cycle checkpoint protein expression and the activation of caspase-9 and caspase-3 in the total cell lysate of OEL-treated U87 cells. Cells treated with OEL (0, 10, 20, and 30 μmol/L) for 24 h were subjected to Western blotting. (A) OEL had no effect on the levels of cdc2, but enhanced the levels of p-cdc2 (Thr14, Tyr15) and decreased cyclin B1 in U87 total cells lysates. (B) OEL induced the activation of caspase-9 and caspase-3 in U87 cells.

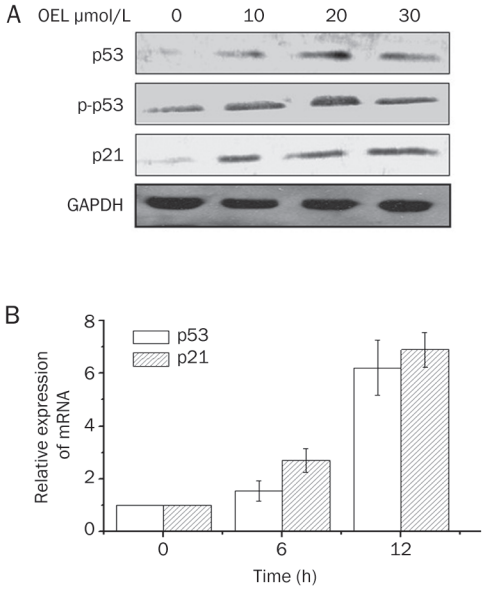

Figure 6. (A) Western blot analyses of p53 and $p21^{Waf1/Cip1}$ expression in OEL-treated U87 total cell lysates. (B) Relative expression of p53 and $p21^{Waf1/Cip1}$ mRNA in U87 cells. The cells were treated with or without 30 μmol/L OEL for 6 and 12 h. Relative expression of p53 and $p21^{Waf1/Cip1}$ mRNA were determined by quantification after real-time PCR. RNA levels (normalized to GAPDH RNA levels) are represented as the fold increase or decrease relative to the control strain. Data are expressed as mean±SD of three independent experiments.

(Figure 5). These results show that OEL exposure induces DNA damage, thereby causing cell cycle arrest and apoptosis.

OEL upregulates the expression levels of p53 and $p21^{Waf1/Cip1}$

Western blot analysis and RT-PCR analysis revealed that the mRNA and protein levels of p53 and $p21^{Waf1/Cip1}$ were upregulated markedly after 6 h to 12 h treatment with OEL (Figure 6A and 6B).

OEL-induced cell cycle arrest and apoptosis are dependent on p53 function

To examine the contribution of p53 to OEL-induced cell death, we monitored cell viability with or without PFT-α, a specific inhibitor of p53 transcriptional activity, in the absence or presence of OEL in U87 and A172 cells. Pretreating cells with 10 μmol/L to 30 μmol/L of PFT-α blunted the inhibitory effect of OEL on cell viability and partially reversed the OEL-induced apoptosis in U87 (Figure 7A and 7C) and A172 cells (Figure 7B and 7D). In addition, OEL-induced apoptosis in U251 (mutant p53) and Saos-2 cells (p53 deficient) were examined. OEL-induced apoptosis was less dramatic in U251 and Saos-2 cells than in U87 and A172 cells (Figure 8A and 8B). These data show that OEL-induced apoptosis is dependent on p53 function.

U251 and Saos-2 cells were stained with PI and analyzed by flow cytometry to confirm that p53 plays a crucial role in OEL-induced G_2/M arrest. In response to OEL treatment, U251 (Figure 8C and 8E) and Saos-2 (Figure 8D and 8F) cells did not accumulate in G_2/M phase compared to U87 and A172

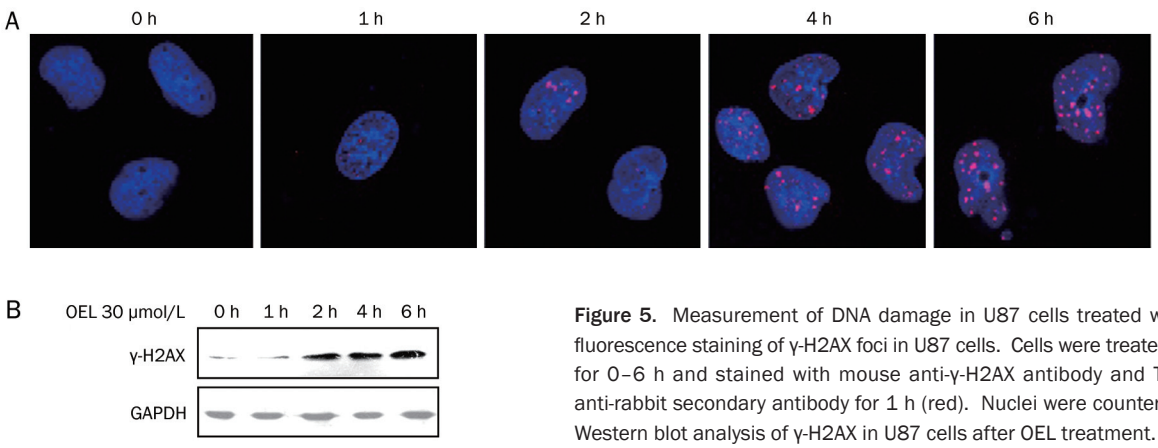

Figure 5. Measurement of DNA damage in U87 cells treated with OEL. (A) Immunofluorescence staining of γ-H2AX foci in U87 cells. Cells were treated with OEL (30 μmol/L) for 0–6 h and stained with mouse anti-γ-H2AX antibody and TRITC-conjugated goat anti-rabbit secondary antibody for 1 h (red). Nuclei were counterstained with DAPI. (B) Western blot analysis of γ-H2AX in U87 cells after OEL treatment.

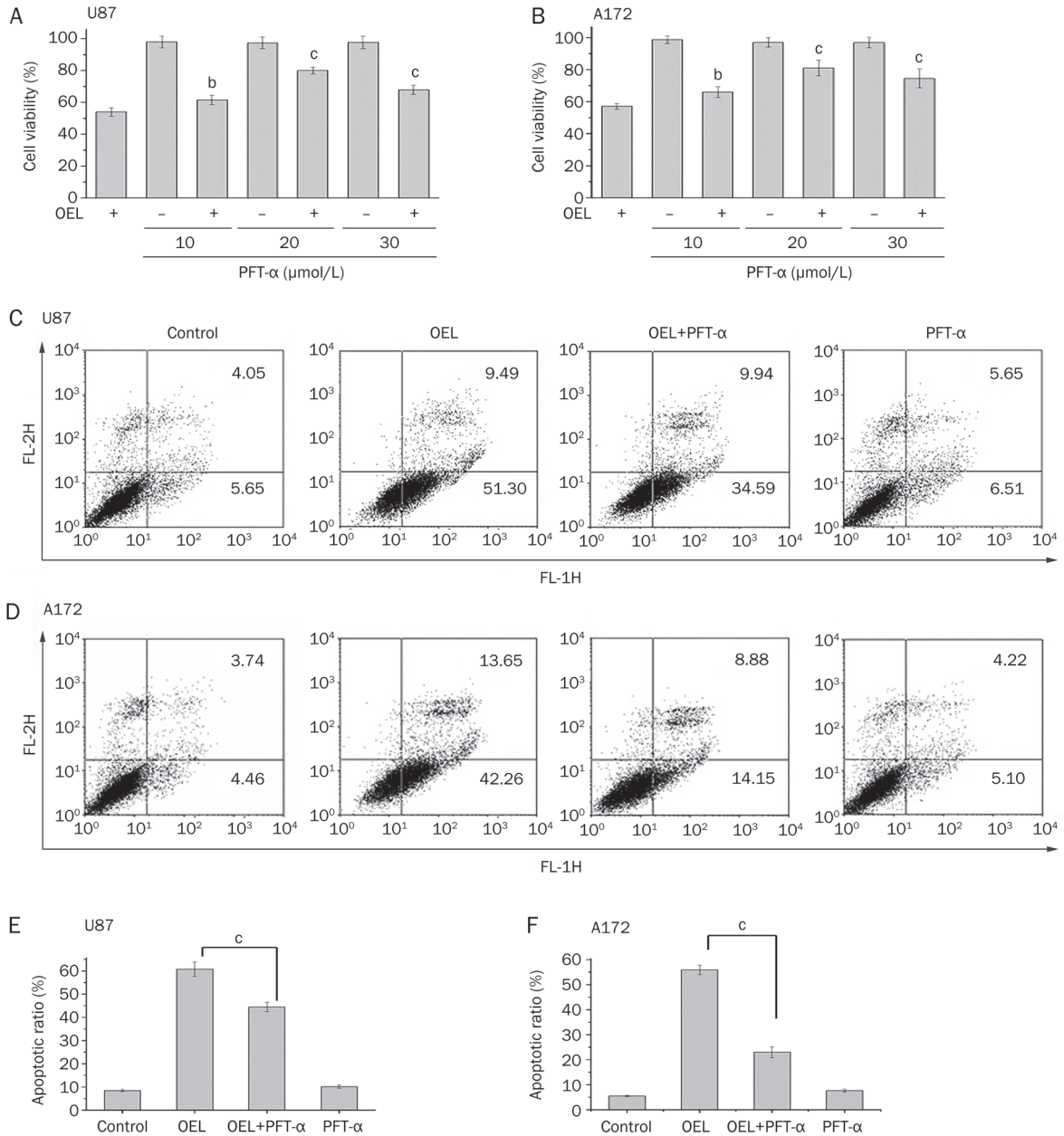

Figure 7. Effects of PFT-α on the OEL-induced reduction of cell viability and increased apoptosis in U87 and A172 cells. The cells were treated with 30 μmol/L OEL for 24 h in the presence or absence of 10–30 μmol/L PFT-α. The cell viability ratio (A, B) and the apoptotic ratio (C, D, E, F) were measured by MTT and flow cytometric analysis. $^{b}P<0.05$, $^{c}P<0.01$ compared with OEL alone group. Data are expressed as the mean±SD of three independent experiments.

cells. We also investigated changes in the cell cycle distribution, with or without PFT-α (specific inhibitor of p53 transcriptional activity), in the absence or presence of OEL in U87 and A172 cells. The p53-specific transcriptional inhibitor, PFT-α, partially reversed the effect of OEL on G_2/M arrest, as shown in Figure 9. These results further confirm that OEL-induced G_2/M arrest is dependent on p53 function.

Discussion

1-Oxoeudesm-11(13)-eno-12,8a-lactone (OEL) (Figure 1A) is a novel, eudesmane-type sesquiterpene compound that exhibits anti-cancer properties. The main goals of the present study were to demonstrate the anti-cancer properties of OEL and delineate the underlying mechanisms of action. Here, we demonstrate that OEL affects glioblastoma cell growth by interfering with cell-cycle progression and inducing apoptosis. The signaling pathways by which OEL exerts its biological effect were also investigated in detail.

OEL significantly reduced the viability of U87 and A172 glioblastoma cells in a concentration- and time-dependent

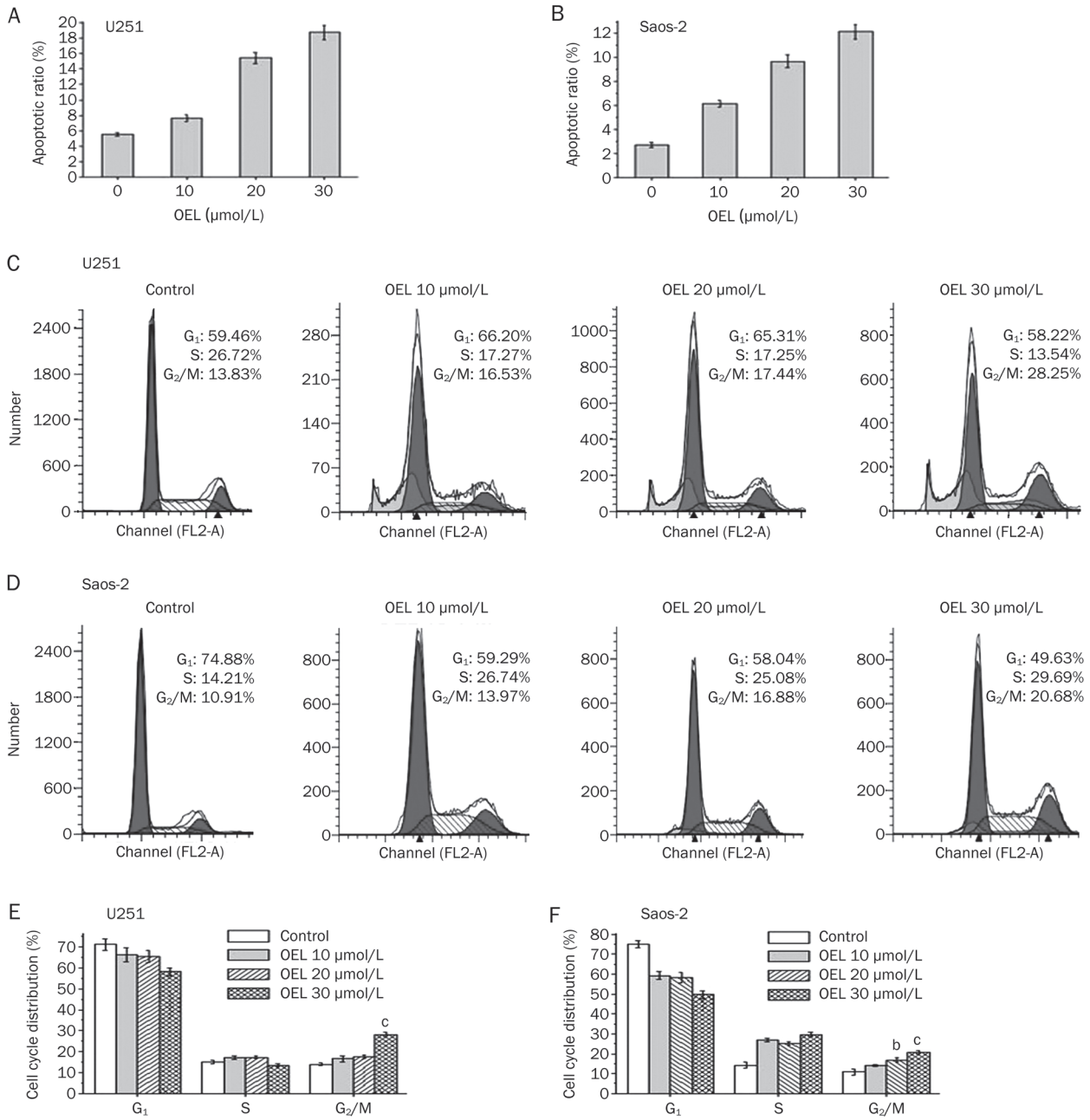

Figure 8. OEL-induced effects were observed in U251 (mutant p53 glioblastoma cell line) and Saos-2 (p53 deficient osteosarcoma cell line). (A, B) OEL induced apoptosis in U251 and Saos-2 cells. (C, D) OEL-induced cell cycle arrest was assessed by flow cytometric analysis in U251 and Saos-2 cells. Corresponding histograms of cell cycle distribution (E, F). $^{b}P<0.05$, $^{c}P<0.01$ compared with the control group.

manner. As revealed by immunofluorescence, OEL-treated cells displayed obvious cellular features of apoptosis. Moreover, quantitative analysis of phosphatidylserine externalization using Annexin V-FITC and PI staining indicated that the population of Annexin V-positive cells increased after OEL treatment. This phenomenon confirmed that OEL induces apoptosis in U87 and A172 glioblastoma cells.

Cell cycle interference is one of the most important mechanisms implicated in the cytotoxic effects and apoptosis of anticancer drugs[20]. Flow cytometric results showed that treating glioblastoma cell lines with OEL significantly inhibited cell cycle progression and arrested cells in G_2/M phase. During the cell cycle, the G_2/M checkpoint is a potential target for cancer therapy that prevents DNA-damaged cells from entering mitosis and allows the repair of DNA that was damaged in late S or G_2 phases, prior to mitosis[21]. The cyclin B/cdc2 complex was originally defined as the maturation-promoting factor. The activity of the complex is controlled in the G_2/M phase and is required for entry into mitosis in eukaryotes. During G_2 phase, cyclin B/cdc2 is inactivated by the phospho-

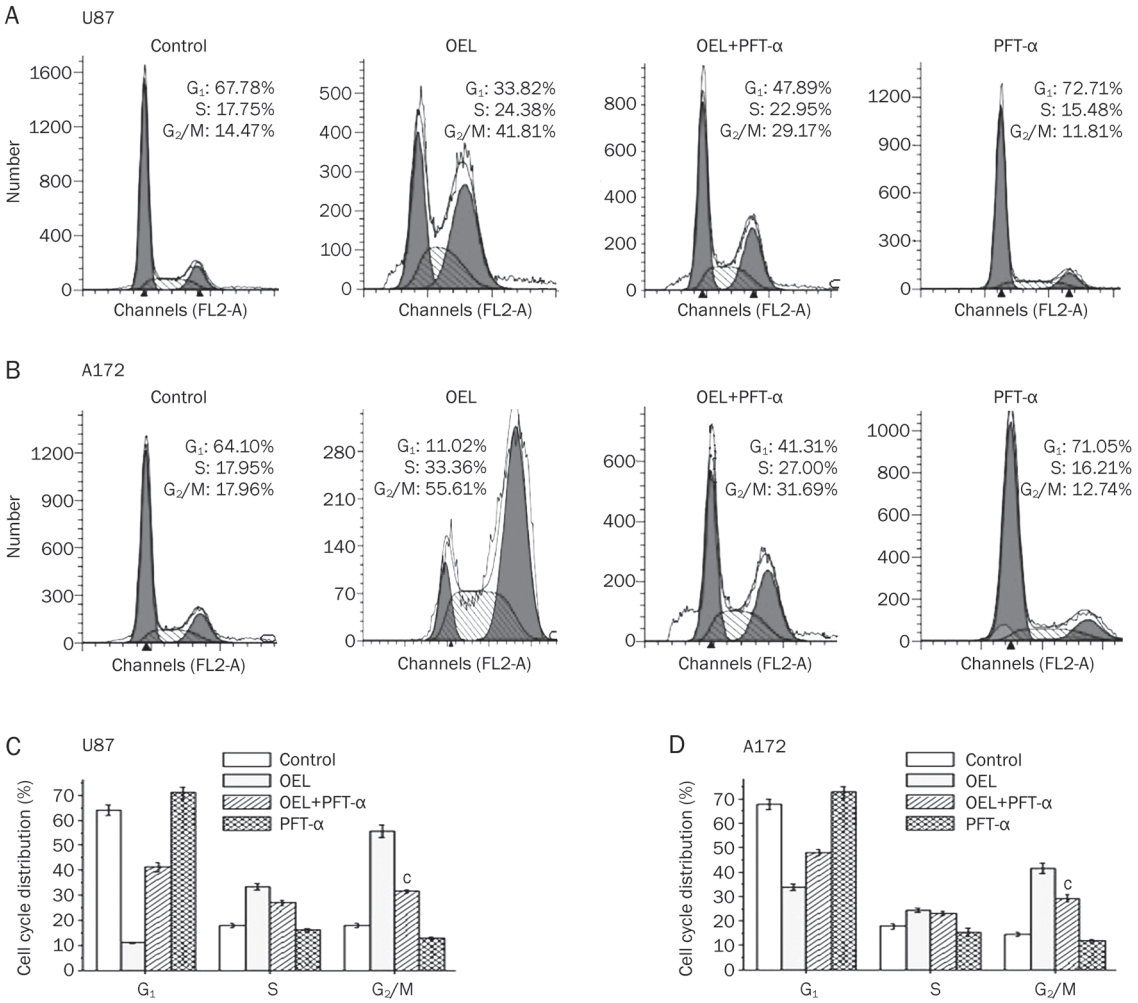

Figure 9. Effects of PFT-α on OEL-induced cell cycle arrest in G_2/M phase in U87 and A172 cells. (A, B) The cells were treated with 30 μmol/L OEL for 24 h in the presence or absence of 20 μmol/L PFT-α. The cell cycle distribution was assessed by flow cytometric analysis. Corresponding histograms of the cell cycle distribution (C, D). $^bP<0.05$, $^cP<0.01$ compared with control group. Data are expressed as the mean±SD of three independent experiments.

rylation of two regulatory residues, Thr14 and Tyr15. Dephosphorylation of Thr14 and Tyr15 by cdc25c in late G_2 phase activates the cyclin B/cdc2 complex and triggers the initiation of mitosis[22, 23]. We examined variations in the expression of key proteins that are involved in the regulation of the cell cycle to elucidate the mechanism by which OEL induces G_2/M arrest. We monitored cdc2 status after treatment with various concentrations of OEL and observed an elevation in the inhibitory phosphorylation of cdc2 (p-cdc2) after treatment, while the total levels of cdc2 were unchanged. Alternatively, cyclin B1 protein levels showed a different kinetic behavior, with a reduction after 24 h. Hence, the elevation in cdc2 phosphorylation and the reduced cyclin B1 expression suggest that OEL-induced G_2/M phase arrest in U87 glioblastoma cells is mediated by the inhibition of cdc2 activity. The arrest of cell cycle progression in G_2/M phase provides an opportunity for cells to either undergo repair mechanisms or follow the apoptotic pathway.

Studies have demonstrated that p53 is an important tumor suppressor protein that acts as a nuclear transcription factor and transactivates multiple genes involved in apoptosis, cell cycle regulation, and numerous other processes[6, 17, 24]. In the present study, we show that OEL potently increased p53 phosphorylation and the mRNA expression levels of p53 and $p21^{Waf1/Cip1}$, which is a major transcriptional target of p53. Our results revealed that the induction of apoptosis and decrease in cell viability in response to OEL were less dramatic in U251 (mutant p53) and Saos-2 (p53 deficient) cells than in U87 and A172 cells. Furthermore, the p53-specific transcriptional inhibitor, PFT-α, partially reversed the effect of OEL on U87 and A172 cell proliferation and apoptosis. Therefore, functional p53 is required for OEL-mediated inhibition of cell growth.

P53 contributes to the maintenance of DNA integrity and regulates mitotic spindle checkpoints that prevent DNA synthesis before chromosome segregation[25]. In addition, $p21^{Waf1/Cip1}$ is a cyclin-dependent kinase inhibitor that is

essential in all phases of cell cycle[26]. CyclinB1 is the regulatory subunit of the cdc2 kinase and is required for the initiation of mitosis. In this study, OEL induced $p21^{Waf1/Cip1}$ and reduced cyclinB1, thereby causing cell cycle arrest in G_2 phase. Moreover, OEL-induced G_2/M phase arrest can be partially reversed by specific p53 inhibitors; however, the effects are less obvious in U251 cells (mutant p53) and Saos-2 cells (p53 deficient) than in U87 and A172 cells (wild-type p53). These findings indicate that the activation of $p21^{/WAF1}$ through the p53 pathway is responsible for the OEL-induced blockade of cell cycle progression.

DNA damage is one of the molecular events associated with cell cycle arrest and apoptosis, and several anti-cancer reagents induce DNA damage[27]. In the present study, OEL caused DNA damage after a 2 h treatment, as evidenced by the formation of γ-H2AX foci and an increase in γ-H2AX protein levels. p53 triggers a variety of cell cycle-regulatory events to limit the proliferation of damaged cells in response to DNA damage. Then, a p53-controlled cell cycle begins with increased expression of the p21 proteins, arresting cells in G_2/M phase and providing time for DNA repair[28]. However, p53 proteins activate the transcription of a variety of apoptosis-associated genes when DNA damage exceeds the repair capacity of the cell, inducing apoptosis[29].

p53 can also enhance the transcription of the pro-apoptotic BH3-only proteins, Noxa and Puma, which indirectly promote Bax activation by inhibiting the function of the anti-apoptotic proteins, Bcl-2 or Bcl-xL[30], and results in mitochondrial membrane permeabilization and the release of cytochrome *c*, leading to apoptosis and caspase activation. The present study demonstrates that OEL activated caspases-9 and -3 in U87 cells, which supports a role for the caspase-activated pathway for OEL-induced apoptosis in glioblastoma cells.

In this study, OEL has growth inhibitory effects on glioblastoma cells. U87 and A172 cells (p53 wild-type) exhibited a higher sensitivity to OEL than U251 (mutant p53) and Saos-2 (p53 deficient). OEL was less cytotoxic to normal cells compared with tumor cell lines, suggesting that this compound is promising for the treatment of glioblastoma.

Therefore, OEL inhibits glioblastoma U87 and A172 cell proliferation through DNA damage, which further triggers p53 activation and induces p53-dependent cellular responses, including cell cycle arrest and apoptosis. The current status and future advancement of OEL will be useful for the development of chemotherapeutic agents against glioblastoma.

Acknowledgements

This work was supported by grants from National Natural Science Foundation of China (No 81273532) and the Shandong Provincial Natural Science Foundation No 2009ZRB02091).

Author contribution

Prof Xia LI designed the research and revised the manuscript; Shan-shan LIU conducted the research, analyzed the data, and wrote the paper; Yan-feng WANG, Li-sha MA, Bei-bei ZHENG, Lin LI, and Wei-dong XIE helped with portions of the research.

References

1 Tabatabai G, Wick W, Weller M. Stem cell-mediated gene therapies for malignant gliomas: a promising targeted therapeutic approach? Discov Med 2011; 11: 529–36.
2 Liu G, Black KL, Yu JS. Sensitization of malignant glioma to chemotherapy through dendritic cell vaccination. Expert Rev Vaccines 2006; 5: 233–47.
3 Sakariassen PO, Immervoll H, Chekenya M. Cancer stem cells as mediators of treatment resistance in brain tumors: status and controversies. Neoplasia 2007; 9: 882–92.
4 Hu W, Kavanagh JJ. Anticancer therapy targeting the apoptotic pathway. Lancet Oncol 2003; 4: 721–9.
5 Pae HO, Oh GS, Choi BM, Seo EA, Oh H, Shin MK, *et al*. Induction of apoptosis by 4-acetyl-12,13-epoxyl-9-trichothecene-3,15-diol from *Isaria japonica* Yasuda through intracellular reactive oxygen species formation and caspase-3 activation in human leukemia HL-60 cells. Toxicol *In Vitro* 2003; 17: 49–57.
6 Li X, Zhao Y, Wu WK, Liu S, Cui M, Lou H. Solamargine induces apoptosis associated with p53 transcription-dependent and transcription-independent pathways in human osteosarcoma U2OS cells. Life Sci 2011; 88: 314–21.
7 Meng XW, Lee SH, Kaufmann SH. Apoptosis in the treatment of cancer: a promise kept? Curr OpinCell Biol 2006; 18: 668–76.
8 Reed JC. Apoptosis-targeted therapies for cancer. Cancer Cell 2003; 3: 17–22.
9 Jung MJ, Yoo YC, Lee KB, Kim JB, Song KS. Isolation of epi-oleanolic acid from Korean mistletoe and its apoptosis-Inducing activity in tumor cells. Arch Pharm Res 2004; 27: 840–4.
10 Kim S, Moon A. Capsaicin-induced apoptosis of H-ras-transformed human breast epithelial cells is Rac-dependent via ROS generation. Arch Pharm Res 2004; 27: 845–9.
11 Wang W, Bu B, Xie M, Zhang M, Yu Z, Tao D. Neural cell cycle dysregulation and central nervous system diseases. Prog Neurobiol 2009; 89: 1–17.
12 Wiseman LR, Markham A. Irinotecan. A review of its pharmacological properties and clinical efficacy in the management of advanced colorectal cancer. Drugs 1996; 52: 606–23.
13 Perez EA. Microtubule inhibitors: Differentiating tubulin-inhibiting agents based on mechanisms of action, clinical activity, and resistance. Mol Cancer Ther 2009; 8: 2086–95.
14 Xie WD, Weng CW, Niu YF, Lai PX, Row KH. Eudesmane sesquiterpenes and other constituents from *Aster himalaicus*. Chem Biodivers 2010; 7: 221–4.
15 Dhar SK, St Clair DK. Nucleophosmin blocks mitochondrial localization of p53 and apoptosis. J Biol Chem 2009; 284: 16409–18.
16 Schuler M, Bossy-Wetzel E, Goldstein JC, Fitzgerald P, Green DR. p53 induces apoptosis by caspase activation through mitochondrial cytochrome c release. J Biol Chem 2000; 275: 7337–42.
17 Li X, Wu WK, Sun B, Cui M, Liu S, Gao J, *et al.* Dihydroptychantol A, a macrocyclic bisbibenzyl derivative, induces autophagy and following apoptosis associated with p53 pathway in human osteosarcoma U2OS cells. Toxicol Appl Pharmacol 2011; 251: 146–54.
18 Norbury CJ, Zhivotovsky B. DNA damage-induced apoptosis. Oncogene 2004; 23: 2797–808.
19 Rogakou EP, Boon C, Redon C, Bonner WM. Megabase chromatin domains involved in DNA double strand breaks *in vivo*. J Cell Biol 1999; 146: 905–16.
20 Elledge SJ. Cell cycle checkpoints: preventing an identity crisis.

Science 1996; 274: 1664–72.
21 Wang Y, Ji P, Liu J, Broaddus RR, Xue F, Zhang W. Centrosome-associated regulators of the G(2)/M checkpoint as targets for cancer therapy. Mol Cancer 2009; 8: 8.
22 Jacobs T. Control of the cell cycle. Dev Biol 1992; 153: 1–15.
23 Dash BC, El-Deiry WS. Phosphorylation of p21 in G_2/M promotes cyclin B-Cdc2 kinase activity. Mol Cell Biol 2005; 25: 3364–87.
24 Innocente SA, Abrahamson JL, Cogswell JP, Lee JM. p53 regulates a G2 checkpoint through cyclin B1. Proc Natl Acad Sci U S A 1999; 96: 2147–52.
25 Cross SM, Sanchez CA, Morgan CA, Schimke MK, Ramel S, Idzerda RL, *et al*. A p53-dependent mouse spindle checkpoint. Science 1995; 267: 1353–6.
26 Sancar A, Lindsey-Boltz LA, Unsal-Kacmaz K, Linn S. Molecular mechanisms of mammalian DNA repair and the DNA damage checkpoints. Annu Rev Biochem 2004; 73: 39–85.
27 Cai Y, Lu J, Miao Z, Lin L, Ding J. Reactive oxygen species contribute to cell killing and P-glycoprotein downregulation by salvicine in multidrug resistant K562/A02 cells. Cancer Biol Ther 2007; 6: 1794–9.
28 Yang J, Duerksen-Hughes P. A new approach to identifying genotoxic carcinogens: p53 induction as an indicator of genotoxic damage. Carcinogenesis 1998; 19: 1117–25.
29 Israels ED, Israels LG. The cell cycle. Oncologist 2000; 5: 510–3.
30 Miyashita T, Krajewski S, Krajewska M, Wang HG, Lin HK, Liebermann DA, *et al*. Tumor suppressor p53 is a regulator of bcl-2 and bax gene expression *in vitro* and *in vivo*. Oncogene 1994; 9: 1799–805.